Probing the Structure and Dynamics of a DNA Hairpin by Ultrafast Quenching and Fluorescence Depolarization

Olaf F. A. Larsen, Ivo H. M. van Stokkum, Bas Gobets, Rienk van Grondelle, and Herbert van Amerongen

Division of Physics and Astronomy, Faculty of Sciences, Vrije Universiteit, 1081 HV Amsterdam, The Netherlands

ABSTRACT   DNA hairpins have been investigated in which individual adenines were replaced by their fluorescent analog 2-aminopurine (2AP). The temperature dependence of the time evolution of polarized emission spectra was monitored with picosecond time resolution. Four isotropic decay components for each oligonucleotide indicated the coexistence of at least four conformations. The fluorescence for three of these was significantly quenched, which is explained by hole transfer from 2AP to guanine(s). An ~8-ps component is ascribed to direct hole transfer, the ~50-ps and ~500-ps components are ascribed to structural reorganization, preceding hole transfer. At room temperature, a fraction remains unquenched on a 10-ns timescale, in contrast to higher temperatures, where the flexibility increases. Besides quenching due to base stacking, a second quenching process was needed to describe the data. Evidence for both intrastrand and interstrand hole transfer was found. The extracted probability for stacking between neighboring bases in double-stranded regions was estimated to be ~75% at room temperature and ~25% at 80°C, demonstrating structural disorder of the DNA. Fluorescence depolarization revealed both local dynamics of the DNA and overall dynamics of the entire oligonucleotide. Upon raising the temperature, the C-N terminus of the hairpin appears to melt first; the rest of the hairpin denatures above the average melting temperature.

INTRODUCTION

The dynamics, flexibility, and structure of biomolecules are intimately related, and they are determined by the biomolecular energy landscapes (Frauenfelder et al., 1991). In addition, these landscapes determine structural heterogeneity and disorder of the biomolecules. For DNA, the flexibility has been shown to be important for many processes, such as protein binding (Hogan and Austin, 1987), transcription (Wolffe, 1994; Grove et al. 1996), and packaging of DNA into chromatin (Richmond et al., 1984; Hagerman, 1988). The dynamics of DNA encompasses a wide time scale and ranges from (sub)picoseconds up to milliseconds (Schurr et al., 1992). The dynamical behavior of DNA has been demonstrated by numerous experimental results (e.g., Guest et al., 1991; Parkhurst and Parkhurst, 1995; Georghiou et al., 1996; Naimushin et al., 2000) and may in principle be linked to molecular dynamics simulations (e.g., Briki et al., 1995; Bruant et al., 1999).

Time-resolved fluorescence depolarization has been shown to be an important technique to study the dynamical properties of DNA (Schurr et al., 1992). However, the natural bases of DNA possess very low quantum yields (Cantor and Schimmel, 1980). Very often, fluorescent dyes are either covalently or noncovalently attached to the DNA (e.g., Parkhurst and Parkhurst, 1995, Eggeling et al. 1998). These dyes will obviously perturb the natural structure and dynamics of the DNA. Therefore, selective introduction of

nonperturbing fluorescent base analogs is highly desirable. The fluorescent adenine analog 2-aminopurine (2AP) is a very attractive probe, and its applicability for studying structural and dynamical aspects of DNA and RNA has been demonstrated by several studies (e.g., Nordlund et al., 1989; Wu et al., 1990; Guest et al., 1991; Hochstrasser et al., 1994; Nordlund et al., 1993; Lacourciere et al., 2000). The 2AP probe has several attractive properties. It is incorporated in B-DNA without significantly changing its structure, it base pairs with thymine (Sowers et al., 1986; Nordlund et al., 1989), and its spectral properties are very well characterized (Broo, 1998; Broo and Holmén, 1996; Holmén et al., 1997). The lowest-energy absorption band lies outside the absorption spectrum of DNA/RNA, allowing selective excitation of 2AP. The molecular structures of both adenine (6-aminopurine) and 2AP are shown in Fig. 1.

In general, the studies on homogeneous DNA preparations using 2AP revealed both overall dynamics of the DNA as well as internal dynamics. Interestingly, several isotropic fluorescence times were found to coexist, indicating structural heterogeneity of the DNA. Molecular dynamics studies on DNA molecules containing 2AP showed that during large-scale motions the hydrogen bonds of the 2AP-T and A-T base pairs remain intact (Nordlund et al., 1989). Experimentally, it was observed that several isotropic decay components were significantly quenched (Nordlund et al., 1989; Guest et al., 1991), which was assumed to be associated with the degree of stacking of the bases. Later studies suggest that this quenching might occur due to hole transfer from the 2AP to nearby guanines (Kelley and Barton, 1999). This nucleotide analog has now been shown to be involved in hole transfer in combination with guanine upon ionization through two-photon absorption (Shafirovich et al., 1999, 2000). Recent results by Wan et al. (1999) on DNA preparations with intercalated ethidium bromide suggest

Address reprint requests to Dr. Olaf F. A. Larsen, Division of Physics and Astronomy, Faculty of Sciences, Vrije Universiteit, De Boelelaan 1081, 1081 HV Amsterdam, The Netherlands. Tel.: 31-20-4447931; Fax: 31-20-4447999; E-mail: olaf@nat.vu.nl.
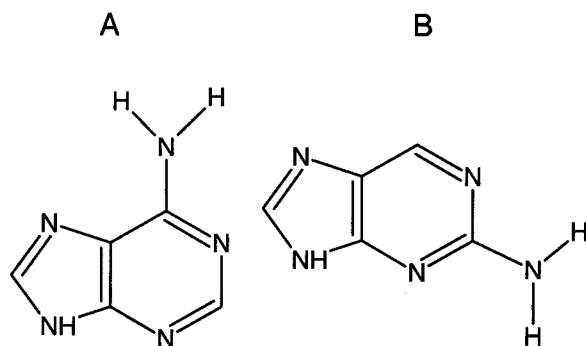
A B

FIGURE 1 Molecular structures of adenine (*A*) and 2AP (*B*).

that fast isotropic decay components (several picoseconds) are associated with direct hole transfer from the probe to the guanine look-alike 7-deazaguanine, whereas slower components reflect structural dynamics of bases that reorient themselves into favorable positions (stacking) after which quenching can occur. The probability that all the bases are favorably stacked decreases when the hole donor and acceptor are positioned at longer distances from each other, which should result in a decreased contribution of the fastest component. Such a decrease was indeed observed experimentally (Wan et al., 1999), whereas the quenching rate remained almost unaltered.

In this work, temperature-dependent picosecond polarized fluorescence measurements on 2AP-substituted DNA hairpins are performed. These DNA hairpins (see Fig. 2) are analogs of Rev binding element 3 (RBE3) (Peterson and Feigon, 1996), an RNA hairpin that contains the high-affinity binding site for the so-called Rev (regulator of the expression of virion proteins) peptide of HIV-1. Binding of Rev to this high-affinity binding site plays a crucial role in the regulation of protein synthesis for the virus (Kingsman and Kingsman, 1996). The structure of the RBE3 RNA hairpin has been determined by NMR (Peterson and Feigon, 1996). It is rich in interesting structural elements such as

non-Watson-Crick base pairs (base pairs G5-A26 and G6-G24), looped-out nucleotides (bases A21 and U25, T25 in our DNA analog), and a loop region (bases T13 to G16). In this study, we aim to monitor the structural dynamics as well as the structural heterogeneity and disorder of the DNA analog of this hairpin. The present study also sets the basis for future research on the structural and dynamical aspects of the RNA hairpin and its complex with the Rev peptide. Future questions that we would like to tackle are how the peptide binding alters the structure, the structural disorder, and the dynamics of the RNA.

MATERIALS AND METHODS

Samples

The DNA oligodeoxynucleotides containing 2AP were obtained from Biolegio (Malden, The Netherlands), and the purity was >99%. 2AP and 2AP-riboside (2APR) were obtained from Sigma (Zwijndrecht, The Netherlands). Each DNA preparation was dissolved in a 10 mM K_2HPO_4/KH_2PO_4 buffer (pH 7.5) with 100 mM KF, pH 7.3. To force the oligodeoxynucleotides in the hairpin structure similar to the RBE3 structure that has been elucidated before (Peterson and Feigon, 1996), each DNA solution was kept at 80°C for 2 min and immediately put on ice afterwards.

The presumed structures of the DNA hairpins are given in Fig. 2. The following oligodeoxynucleotides were synthesized: DNA2AP10, RBE3 DNA analog with the adenine at position 10 substituted by 2AP; DNA2APIN, RBE3 DNA analog with the adenine at position 10 substituted by 2AP, and the guanines at positions 8, 11, 16, 17, 20, 23 substituted by inosines; DNA2AP21, RBE3 DNA analog with the adenine at position 21 substituted by 2AP; DNA2AP26, RBE3 DNA analog with the adenine at position 26 substituted by 2AP; and DNA2AP28, RBE3 DNA analog with the adenine at position 28 substituted by 2AP.

Melting curves

DNA melting curves were determined for all DNA preparations by measuring the temperature dependence of the absorption spectra, using an absorption spectrophotometer (Cary 50 Bio, Varian, Middelburg, The Netherlands), with a temperature-controlled cuvette holder. The melting temperatures were determined by global analysis of the complete absorption spectra as a function of temperature using the model described elsewhere (van Stokkum et al., 1995).

Fluorescence streak-camera measurements

Streak-camera fluorescence images of the different DNA preparations were measured at room temperature (24°C), at melting temperature (58°C), and at 80°C (completely denatured DNA). Because DNA2APIN has a different melting behavior, the following temperatures were used for this oligodeoxynucleotide: 20°C, 35°C (melting temperature), and 80°C. Streak-camera images of 2AP and 2APR were measured at 24°C. Excitation was performed by the frequency-doubled output of an optical parametric amplifier (Coherent, Santa Clara, CA), which was pumped by an amplified titanium-sapphire laser (Coherent). The excitation wavelength was 326 nm (repetition rate, 40 kHz; pulse length, ~100 fs), and its polarization (vertical or horizontal) was adjusted by a Berek polarization compensator. By placing a Glan-Thompson polarizer before the entrance slit of the spectrograph only the vertically polarized emission light was detected. The emission light was then led into a spectrograph (Chromex) and measured using a streak-camera system (Hamamatsu) coupled to a CCD camera
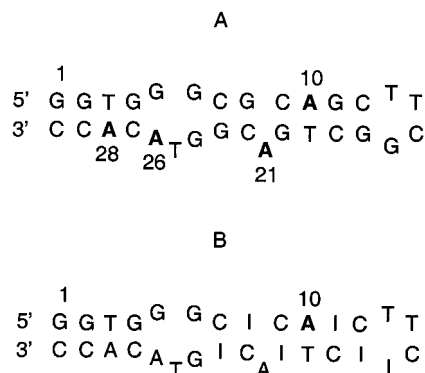

FIGURE 2 Presumed structures of the studied DNA hairpins with 2AP at, respectively, position 10, 21, 26, and 28 (*A*) and the hairpin with 2AP at position 10 with inosine substitutions (*B*).

(Hamamatsu, Herrsching, Germany) (Kleima et al., 2000). The spectral resolution was ~8 nm.

Streak-camera data fitting

With each polarization condition three different time bases were used: 200 ps, 800 ps, and 2200 ps. The instrument response function was modeled using a Gaussian. The full width at half-maximum of the instrument response function depended upon the time base and ranged from 4 to 25 ps. Thus, at a certain temperature each sample resulted in six data sets ($>10^5$ data points) that were simultaneously analyzed using <120 parameters. The contribution of the Raman light from the solvent has been included in the data analysis and has been used to determine the time response of the setup. All obtained isotropic and anisotropic decay times (with their corresponding amplitudes) have a precision better than 10%, except the decay times that possess a very small amplitude ($<1\%$; see tables).

The data have been analyzed using a global analysis method (van Stokkum et al., 1994). The two fluorescence components $I_{VV}(t)$ and $I_{HV}(t)$ (vertically and horizontally polarized excitation) were described by:

$$\begin{bmatrix} I_{VV}(t) \\ I_{HV}(t) \end{bmatrix} = \begin{bmatrix} I_{MA}(t) \times (1 + 2r(t)) \\ I_{MA}(t) \times (1 - r(t)) \end{bmatrix} \otimes I(t), \quad (1)$$

where $I_{MA}(t)$ is the magic angle (isotropic) signal, and $r(t)$ is the anisotropy. $I(t)$ reflects the instrument response and $\otimes$ denotes convolution.

The magic-angle decay, $I_{MA}(t)$, is described by a sum of decays, each component i having its own decay-associated spectrum $A_i(\lambda)$ and rate constant of fluorescence k_i:

$$I_{MA}(t) = \sum_{i=1}^{n} A_i(\lambda) e^{-k_i t} \quad (2)$$

The anisotropy $r(t)$ is described with a non-associative model as the sum of individual anisotropy components j, each with their own rotational correlation time τ_j and amplitude r_j:

$$r(t) = \sum_{j=1}^{m} r_j e^{-t/\tau_j} \quad (3)$$

This non-associative model resulted in a satisfactory fit. Extensive attempts to fit the data with a more complicated associative model have been carried out. In this model, every magic-angle component is linked to its own unique rotational correlation times, which from a physical point of view is more realistic as compared with the non-associative model described above. However, no realistic fitting parameters could be obtained. A simulation of this model has been carried out and showed that realistic physical results can only be obtained when the signal-to-noise ratio is at least one order of magnitude higher than the signal-to-noise ratio in our measurements. Attempts to link different short rotational correlation times and amplitudes to reduce the degrees of freedom did not result in precise estimates either. Hence, associative fitting of these kinds of data is not feasible considering the signal-to-noise ratio and the high quenching of the fluorescence that is observed. Therefore, the anisotropic fitting parameters resulting from a non-associative model should not be over-interpreted.

RESULTS

Melting behavior

We have designed several oligodeoxynucleotides based on the analogy with RBE3, of which the hairpin structure is known from NMR measurements (Peterson and Feigon, 1996). The absorption spectra of the different
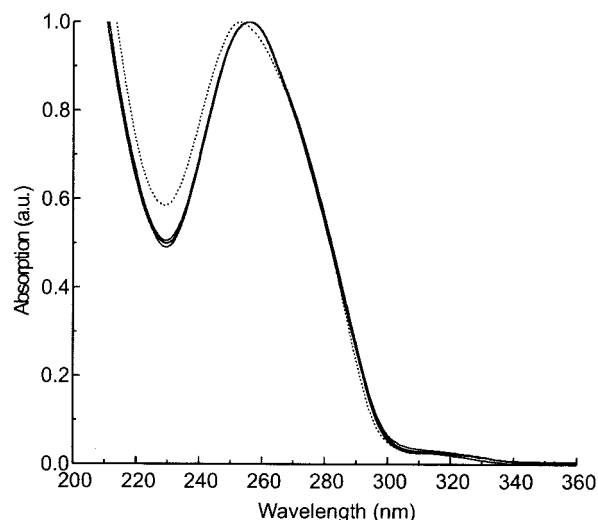

FIGURE 3 Absorption spectra of the studied DNA hairpins. The DNA2APIN spectrum is dotted. The spectra of all other oligonucleotides are indistinguishable from each other.

oligonucleotides are depicted in Fig. 3. Their base content is identical and their spectra are almost indistinguishable except for DNA2APIN, which has a different base composition. In all samples, the weak absorption band around 310 nm is due to 2AP, and in all cases the fluorescence that is monitored originates from this 2AP moiety. A base-pairing scheme for the oligodeoxynucleotides that is based on the analogy with the RBE3 hairpin structure is depicted in Fig. 2. To test whether the different DNA preparations possess the same structure we recorded the absorption spectra as a function of temperature. In Fig. 4 the absorption at 260 nm is plotted for the different oligonucleotides at different temperatures. In all cases a strong (14%) hyperchromism is observed upon going from room temperature to 80°C, reflecting the melting of a structure with many base pairs. Apart from DNA2APIN, all oligonucleotides displayed a very similar melting behavior, and at ~58°C half of the hyperchromism was reached, indicating that roughly 50% of the amount of stacking had been disrupted. We call the corresponding temperature the melting temperature. For DNA2APIN the melting temperature appears to be ~34°C, i.e., 24°C lower. This decrease in melting temperature can be explained by the fact that inosine can only form two H bonds with the opposing cytosine, one less than the guanine it replaces. According to the literature (Lehninger, 1976), such a decrease in number of H bonds should result in a decrease of the melting temperature of ~22°C, very close to the decrease observed here. Therefore, we conclude from the above results that a hairpin structure is formed in all oligonucleotides, with base pairing most likely as in Fig. 2.
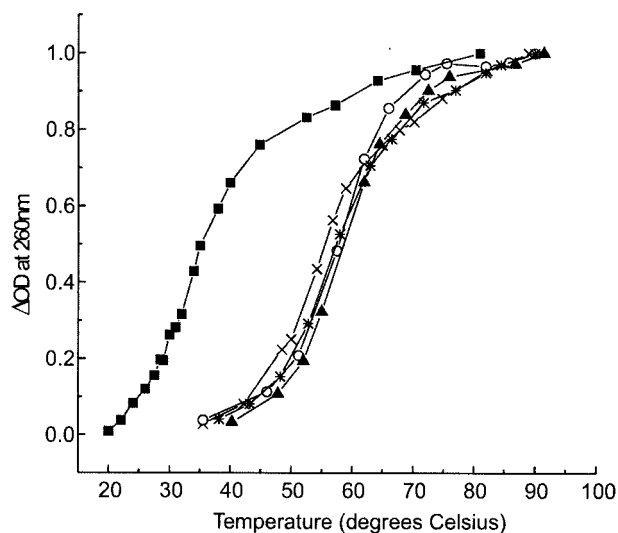
FIGURE 4 Melting curves for the different DNA preparations. Each data point is the difference between the 260-nm absorption at the corresponding temperature and the 260-nm absorption at room temperature; DNA2APIN (■), DNA2AP10 (○), DNA2AP21 (▲), DNA2AP26 (×), and DNA2AP28 (*).

TABLE 1 Isotropic τ_F (in ps) as a function of temperature and contribution to the total signal (%) of the different molecules studied

Molecule, temperature	τ_1 (%)	τ_2 (%)	τ_3 (%)	τ_4 (%)
2AP, 24°C				11×10^3 (100)
2APR, 24°C				10×10^3 (100)
AP10, 24°C	5 (90)	50 (9)		$>1 \times 10^3$ (<0.1)
AP10, 58°C	7 (63)	50 (25)	450 (10)	$>8 \times 10^3$ (1)
AP10, 80°C	11 (45)	70 (30)	430 (24)	$>8 \times 10^3$ (<1)
AP21, 24°C	10 (39)	30 (13)	290 (4)	$>8 \times 10^3$ (44)
AP21, 58°C	10 (53)	90 (12)	500 (13)	$>8 \times 10^3$ (22)
AP21, 80°C	9 (51)	70 (25)	460 (24)	$>8 \times 10^3$ (1)
AP26, 24°C	13 (51)	60 (30)	500 (11)	$>8 \times 10^3$ (8)
AP26, 58°C	16 (47)	90 (25)	640 (25)	$>8 \times 10^3$ (3)
AP26, 80°C	14 (37)	80 (29)	470 (33)	$>8 \times 10^3$ (1)
AP28, 24°C	9 (43)	30 (50)	330 (6)	$>8 \times 10^3$ (1)
AP28, 58°C	14 (40)	90 (33)	540 (25)	$>8 \times 10^3$ (2)
AP28, 80°C	20 (25)	110 (39)	530 (35)	$>8 \times 10^3$ (<1)
APIN, 20°C	20 (16)	130 (38)	460 (41)	$>8 \times 10^3$ (5)
APIN, 35°C	19 (24)	140 (31)	650 (35)	$>8 \times 10^3$ (9)
APIN, 80°C	10 (17)	100 (26)	610 (56)	$>8 \times 10^3$ (1)

All times and amplitudes are within 10% accuracy, except the times with a very low corresponding amplitude ($\leq$1%).

Time-resolved measurements

In Fig. 5 the polarized fluorescence decay curves at 24°C for 2AP and 2APR are shown. The fitting parameters are given in Tables 1 and 2. The isotropic decay time of ±11 (2AP) and ±10 ns (2APR) are close to those presented in the literature (respectively, 11.8 ns and 10.4 ns) (Holmén et al., 1997). Although the time window of our equipment is
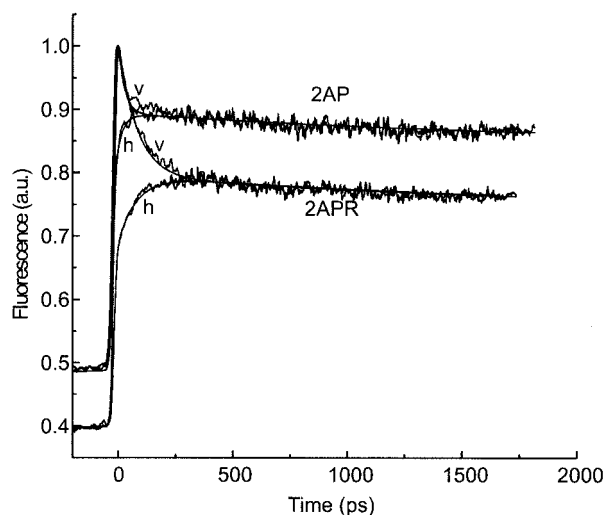

FIGURE 5 Polarized fluorescence-decay curves at 390 nm for 2AP and 2APR at 24°C. Traces obtained for vertically polarized excitation and detection of vertically polarized emission are indicated with a *v*, whereas traces obtained from horizontally polarized excitation and detection of vertically polarized emission are indicated with an *h*. The smooth lines are fits of the data.

2.2 ns, longer fluorescence times can be estimated because of the backsweep of the streak camera (Kleima et al., 2000). The obtained rotational correlation times of 2AP and 2APR are 30 and 80 ps, respectively. The fitted initial anisotropy values of 0.31 and 0.34 are lower than the theoretical maximum of 0.4 and are probably due to solvent relaxation that is also manifested by the large Stokes' shift of 5000 cm^{-1}.

A completely different fluorescence decay and depolarization pattern is observed when 2AP is incorporated in the oligodeoxynucleotides. The most extreme case is observed for DNA2AP10, which is shown in Fig. 6 at room temperature. In DNA2AP10, most of the fluorescence (90%) decays with a time constant of 5 ps, an additional component of 50 ps has a contribution of 9%, and a very small fraction (<0.1%) has a decay time over 1 ns, but the accuracy of this value is limited due to the small corresponding contribution (Table 1) (the percentage is the contribution of the area of the decay-associated spectrum of a component to the sum of areas of all the decay-associated spectra). Upon raising the temperature to 58°C an additional time constant of ~450 ps appears. In addition, the relative contribution of the fastest component decreases, and this decrease becomes even more pronounced at 80°C where the complete hairpin has been melted out. Because the fluorescence spans a larger time window at higher temperatures it is also possible to study the fluorescence depolarization behavior, and the results are given in Table 2. The anisotropy was fitted with two components of 100 ps and 840 ps at 58°C and 40 ps and 250 ps at 80°C (for interpretation see Discussion).

The 2AP fluorescence quenching was supposed to originate from hole transfer from the 2AP probe to nearby

TABLE 2 τ_{R1} and τ_{R2} (in ps) as a function of temperature with amplitudes (r_{01} and r_{02})

Molecule	24°C (20°C)		58°C (35°C)		80°C	
	τ_{R1} (r_{01})	τ_{R2} (r_{02})	τ_{R1} (r_{01})	τ_{R2} (r_{02})	τ_{R1} (r_{01})	τ_{R2} (r_{02})
2AP	30 (0.31)		ND	ND	ND	ND
2APR	80 (0.34)		ND	ND	ND	ND
AP10			100 (0.24)	0.8×10^3 (0.14)	40 (0.18)	250 (0.16)
APIN	20 (0.05)	1.8×10^3 (0.34)	160 (0.12)	1.1×10^3 (0.23)	30 (0.13)	200 (0.22)
AP21	140 (0.20)	1.8×10^3 (0.16)	80 (0.23)	0.9×10^3 (0.12)	40 (0.17)	210 (0.18)
AP26	150 (0.12)	2.0×10^3 (0.26)	60 (0.15)	420 (0.21)	30 (0.17)	200 (0.19)
AP28	230 (0.23)	2.1×10^3 (0.17)	60 (0.17)	370 (0.20)	50 (0.18)	210 (0.16)

All times and corresponding amplitudes are within 10% accuracy. However, these parameters should not be overinterpreted because they are the results of an oversimplified model. Due to the very heavy quenching, the obtained rotational correlation times of DNA2AP10 at 24°C could not be precisely estimated. ND, not determined.

guanines (see also Introduction), which have the lowest oxidation potential of all the natural bases. To test this idea we have replaced the six guanines that are closest to 2AP in DNA2AP10 by inosines which are guanine look-alikes but have an oxidation potential that is unfavorable for hole transfer (DNA2APIN, Fig. 2 *B*). Indeed, we observe a large increase of the fluorescence intensity (at least a factor of 20), consistent with the idea of fluorescence quenching due to hole transfer to guanine (see Fig. 6). The time-resolved measurements are satisfactorily fit with four decay times at all temperatures, and both decay times and corresponding contributions do not vary much (Table 1). It should be noted that at 80°C the contribution of the slowest component is ~1% or even less, and this might be due to the fact that the preparation is not entirely pure (~99% for all oligonucleotides), and we ascribe this to the presence of free 2AP in

solution and small pieces of DNA that resulted from incomplete synthesis.

The other oligonucleotides show more fluorescence quenching than DNA2APIN, and fitting of the time-resolved measurements at all temperatures shows decay times that are roughly similar to the ones observed for DNA2AP10 at 58°C and 80°C, a fast component (<20 ps), two intermediate components, in most cases ~50 ps and ~500 ps, and one component of many nanoseconds. As an example, the decay-associated spectra of DNA2AP21 at 24°C are shown in Fig. 7. However, at room temperature the contribution of the fastest component is in all cases smaller than in the case of DNA2AP10. At 80°C, when all base pairs have disappeared and the oligonucleotides are presumably quite structureless, the decay components (times and contributions) are much more similar for all the DNAs. The isotropic fitting results are given in Table 1.

In all cases, the anisotropy decay could satisfactorily be described by two components (Table 2). The slowest com-
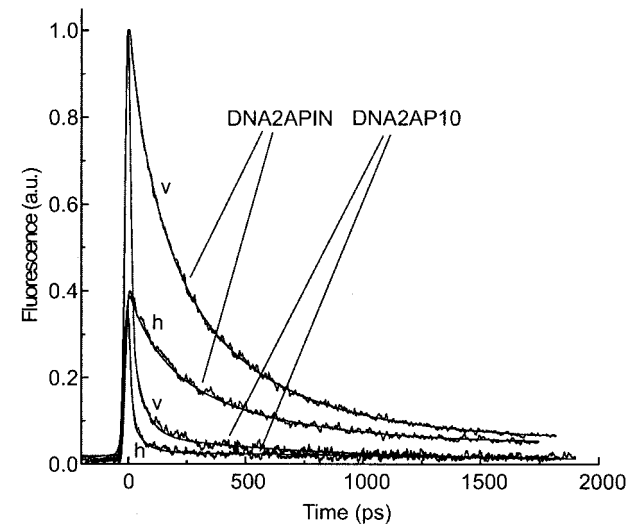

FIGURE 6 Time-resolved fluorescence traces for DNA2AP10 and DNA2APIN at room temperature at 390 nm. Traces obtained for vertically polarized excitation and detection of vertically polarized emission are indicated with a *v*, whereas traces obtained for horizontally polarized excitation and detection of vertically polarized emission are indicated with an *h*. The smooth lines are fits of the data.
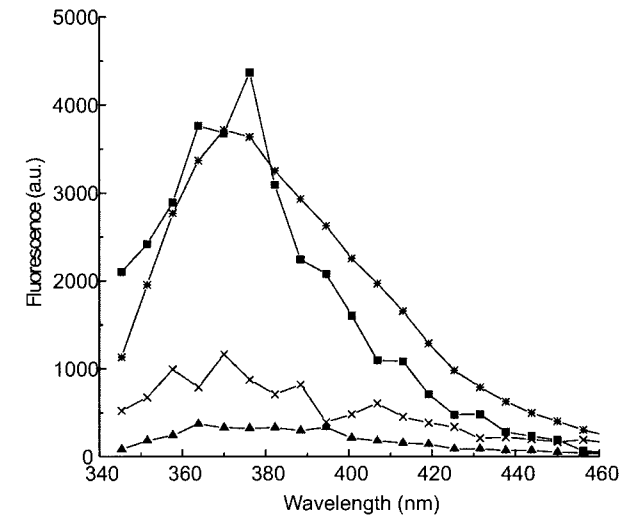

FIGURE 7 Magic-angle decay-associated spectra at 24°C of DNA2AP21. The corresponding decay times are 10 ps (■), 30 ps (×), 0.29 ns (▲), and 9.8 ns (*).

ponent is close to 2 ns in all cases at room temperature and probably reflects the overall motion of the oligodeoxynucleotide together with some bending and twisting motions. The fastest component is of the same order of magnitude for DNA2AP21, DNA2AP26, and DNA2AP28. No significant fast depolarization is observed for DNA2APIN. At the melting temperature the slowest component is considerably faster for DNA2AP26 and DNA2AP28 than for the other oligonucleotides. Also, the τ_{r1} component appears to be faster, although the difference between DNA2AP21, DNA2AP26, and DNA2AP28 may not be significant. At 80°C, both the slowest and the fastest component are very similar (~210 ps and ~40 ps) in all cases (largely disordered structure; see Discussion). However, at lower temperatures it shows more variation due to the different microenvironments in the various complexes.

An important point to note is that no quenching processes that are faster than the time response of our detection setup are missed; the initial intensities (the sum of the decay-associated spectra) of free 2AP and of 2AP incorporated in DNA are identical within experimental error.

DISCUSSION

We have designed a DNA-oligonucleotide that resembles the RBE3 structure as determined before (Peterson and Feigon, 1996) with the intention to form a similar hairpin structure and to incorporate the fluorescent base 2AP at different positions to probe the structural heterogeneity, dynamics, and disorder with time-resolved fluorescence measurements. The temperature-dependent absorption measurements show that indeed a folded structure has been formed with a large number of base pairs, and the observed decrease in melting temperature upon replacing six guanines by six inosines is consistent with the proposed base-pairing scheme in Fig. 2, which is based on the analogy with RBE3. We realize that this consistency does not provide an absolute proof for the assumed base-pairing scheme, but there is no obvious alternative highly folded structure that might occur.

When compared with the fluorescence of free 2AP or 2APR, the time-resolved fluorescence data of all oligonucleotide-2AP complexes show additional short fluorescence decay components that must be due to quenching mechanisms within the oligonucleotides. Following earlier work, this strong quenching of the 2AP fluorescence on a picosecond time scale is to a large extent ascribed to the interaction with guanines (Kelley and Barton, 1999). A plausible explanation for this quenching might be hole transfer, which is known to occur in DNA between ionized 2AP and guanine(s) (Shafirovich et al., 2000). Guanine is the hole acceptor because it has the lowest oxidation potential when compared with the other bases (Steenken and Javonavic, 1997), whereas in this case excited 2AP acts as the hole donor. The fastest isotropic decay time should be due to

hole transfer in which the bridge bases (between the hole donor 2AP and the hole acceptor guanine) are perfectly stacked such that hole transfer can occur. The longer isotropic decay times might in principle originate from conformations in which different H bonds or stacking interactions are present (when compared with the component that decays with the fastest rate). These intermediate components might also originate from conformations with the bases in a position that is unfavorable for the quenching process and require reorganization before the hole transfer process can take place. In that case these intermediate isotropic times would reflect structural dynamics of the DNA hairpins. At high temperatures, the intermediate isotropic times are still observed, making it unlikely that these times are due to conformations with different H bonds, because the latter are presumably absent at 80°C. It seems more likely that the intermediate times reflect structural reorganization. This view is similar to the one adopted by Wan et al. (1999), who claim that some conformations are favorable for direct quenching to occur, whereas other conformations first need to be reorganized before quenching is possible. The long decay time observed in all samples is due to 2AP in a microenvironment that is completely unfavorable for quenching and reflects the natural lifetime of 2AP. This time is difficult to estimate in most cases because of the very small amount of fluorescence light that is present on that timescale. The fact that different decay components are observed for one type of oligonucleotide shows that 2AP does not have one identical rigid conformation in all cases. Apparently, different conformations coexist, which is in line with the data obtained by Guest et al. (1991) and Nordlund et al. (1989). Both groups also studied the time-resolved fluorescence of 2AP-substituted DNA oligodeoxynucleotides. The isotropic fluorescence at 20°C yielded (for each of the different possible counter bases T, G, A, and C) four lifetimes, which on the average were ~50 ps, ~400 ps, ~2 ns, and ~8 ns (Guest et al., 1991). Isotropic fluorescence times of ~100 ps, ~640 ps, ~3.0 ns, and ~8.2 ns were found when 2AP was base paired with another 2AP and ~100 ps, ~680 ps, 3.1 ns, and 9.1 ns when 2AP was base paired with adenine at 25°C (Nordlund et al., 1989). The shortest isotropic time was in both studies attributed to 2AP positioned in a more stacked form, as compared with the longer component(s). However, the shorter (~10-ps) component that we observed was not revealed because of their limited time response. It is surprising that in a recent paper by Wan et al. (2000) in which they studied 2AP-substituted DNA duplexes, only one isotropic decay time was observed, which suggests only one conformation of DNA duplex to be present. This seems to be in contradiction with results obtained earlier by Wan et al. (1999) in which they studied ethidium-bromide-labeled DNA duplexes, as well as with the aforementioned results obtained by Guest et al. (1991), Nordlund et al. (1989), and the results presented in this work. Furthermore, a rate dependence of the charge transfer

TABLE 3 Comparison of the calculated (see Appendix) fast decay time τ_1 and corresponding contribution with experimental data at 80°C

DNA	Calculated contribution τ_1	Experimental contribution τ_1	Calculated decay time fast component (ps)	Experimental decay time fast component (ps)
DNA2AP10	0.49	0.45	10	11
DNA2AP21	0.49	0.51	10	9
DNA2AP26	0.32	0.37	14	14
DNA2AP28	0.28	0.25	20	20

as a function of hole donor-acceptor distance was observed by Wan et al. (2000), which also seems to be in contradiction with the earlier results by Wan et al. (1999) where it was stated that no rate dependence was observed.

High temperatures

At the highest temperature(s) the slowest component is virtually absent in all cases, apart from a very small contribution that may be due to impurities ($\leq 1\%$). This shows that the melting of the tertiary structure removes the energetic barrier between conformations in which quenching either can or cannot take place. At the highest temperatures all or at least most of the base pairs have been disrupted, and we will first discuss the fluorescence data for this situation, when the oligonucleotides adopt (disordered) single-stranded structures. We compare all oligonucleotides that do not have guanines replaced by inosines, because they are most similar in composition. These oligodeoxynucleotides all have similar decay times (on average 15, 85, and 475 ps). The contribution of the fastest component is largest for DNA2AP10 (45%) and DNA2AP21 (51%), which have one guanine as a neighbor and another guanine two bases away. The contribution for DNA2AP26 is 37% (one guanine two bases away and another guanine three bases away in the same direction). Finally, the contribution for DNA2AP28 is 25% (one guanine four bases away and another guanine five bases away in the same direction). This is strongly reminiscent of the results by Wan et al. (1999) where a decrease of the amount of fast quenching of intercalated ethidium bromide fluorescence was observed when Z (7-deazaguanine) was positioned further away, whereas the rate of quenching did not change very much. In addition, they observed another quenching component of many tens of picoseconds, which was ascribed to reorientation of bases leading to base stacking that is suitable for hole transfer. We adopt a similar explanation for our results. 2AP, guanine, and the intervening bases have a finite probability to be favorably stacked for electron transfer in which case fluorescence quenching occurs with a rate that takes several picoseconds and is not strongly dependent on the number of intervening bases. However, the probability that all relevant bases are favorably stacked decreases when the distance between 2AP and guanine increases. This leads to a decrease of the contribution of the fastest quenching component. The slower

quenching times correspond to the times necessary for reorientation or displacement of relevant bases such that hole transfer becomes possible. Alternatively, these slower times correspond to conformations that do not show proper stacking that is favorable for the fastest quenching process but still allow quenching to occur, albeit at a slower rate. However, our anisotropy data show that substantial structural dynamics occurs on a time scale of tens of picoseconds, favoring the former explanation. We have tried to model the contributions and transfer rates for the fastest process, using a few simple assumptions. For detailed calculations see Appendix.

The probability that two neighboring bases instantaneously adopt a mutual orientation/positioning that is favorable for electron transfer is called p_1. When such a situation occurs, the quenching rate k is equal to k_1. The probability that an unfavorable situation occurs is therefore $1 - p_1$, and we assume that quenching is absent, i.e., $k = 0$ ns^{-1}. When guanine is two bases away, the probability that there is a situation that is favorable for electron transfer is p_1^2, and the quenching rate is still k_1. When two guanines are present on both sites of 2AP and when the conformation is favorable for quenching by both guanines, the quenching rate doubles to $2k_1$. When two guanines are present on the same side of 2AP, it is assumed that only the nearest one contributes to the quenching, and again the quenching rate is k_1.

In the case of DNA2AP10 and DNA2AP21, the probability that the guanines on both sides can contribute to fast quenching is p_1^3, and the corresponding rate is $2k_1$ (i.e., the nearest guanines on both sides, 2AP, and the intermediate C are all favorably stacked). The probability that only one guanine contributes is $1 - (1 + p_1)(1 - p_1)^2$, and the quenching rate is k_1 (see Appendix). In our experiment we cannot distinguish between $2k_1$ and k_1 when they are simultaneously present, and a fitting procedure can at most provide an average value. Therefore, we calculated (see Appendix) a weighted average rate, and the contribution is the weighted sum of both contributions above, which should be equal to 0.48 (average of fitted values of 0.45 and 0.51 for DNA2AP10 and DNA2AP21, respectively; see Tables 1 and 3). This means that $p_1 = 0.39$, i.e. a rather low probability of stacking, which might be expected for these unstructured, melted single-stranded oligonucleotides. Using this value of p_1, one expects a contribution of 0.02 (2%) for the fastest quenching process in the case of DNA2AP28,

whereas the fitted value is 0.25. Within the context of the above model this implies that an additional quenching process with probability p_2 must occur that dominates the quenching when guanine is relatively far away. Consequently, the corresponding rate is 50 ns^{-1}, giving rise to the quenching time of 20 ps. This quenching process might for instance be due to a neighboring sugar. It has been shown (Farrer and Thorp, 2000) that the sugar moieties in DNA can also be oxidized. Assuming that both quenching processes can occur for all oligonucleotides in an independent way, we can try to fit the contributions and quenching rates in all four cases (eight experimental parameters, namely, four rates and four contributions) with two probabilities (p_1 and p_2) and two rates (k_1 and k_2). This leads to the following fitted values: $p_1 = 0.25$, $p_2 = 0.28$, $k_1 = 128$ ns^{-1}, and $k_2 = 50$ ns^{-1}, which give a satisfactory fit of the observed contributions and quenching rates (see Table 3, note that the calculated rates are average rates, weighted by the probability that a certain quenching process occurs). This very simple model implies that at high temperatures a neighboring base or a neighboring sugar have similar probability to be favorably positioned for hole transfer and that the hole transfer rates are of the same order of magnitude. The model we developed here is in line with the model as proposed by Wan et al. (1999), but it is more quantitative in our case. In our opinion, the 8-ps time that is observed for the fastest quenching process represents hole injection from the excited 2AP onto the neighboring DNA base. The transfer of the hole over the bases between 2AP and guanine is assumed to occur on a much faster time scale. Of course, the hole can hop back and forth between the 2AP and the bridge. Only when the bases on the bridge are appropriately stacked will the hole move over the bridge to the guanine (on a much faster time scale than 8 ps).

Low temperatures

At room temperature the contribution of the fast quenching process increases dramatically to 90% for DNA2AP10. Using the same model and assuming that p_2 does not change, p_1 becomes 0.72. This implies an increased amount of stacking, which is to be expected in the partly double-stranded hairpin structure. In such a structure, quenching by a neighboring sugar would be less likely and, assuming that p_2 becomes 0, p_1 increases to a value of 0.75. Apparently, even in such a hairpin structure, stacking is not perfect, and there is disorder. Analogous to earlier results (Wan et al., 1999), reorientation of the bases, in DNA2AP10 occurring with a time constant of 50 ps, leads to further quenching (again, a slower quenching process that occurs when the bases are not perfectly stacked might also explain this component). The fact that the fast quenching time decreases from 11 ps to 5 ps suggests that additional quenching processes occur in the hairpin structure, possibly due to hole transfer to the guanines in the opposing strand. A similar

situation occurs for DNA2AP28. Assuming that $p_2 = 0$ one finds $p_1 = 0.81$, very similar to the obtained value for DNA2AP10 (0.75). The fact that for DNA2AP28 the contribution of the fastest component (0.43) is so much lower than for DNA2AP10 (0.90) is within the context of the above model entirely explained by the fact that in the former structure 2AP donates a hole to only one guanine in the same strand, which is relatively far away. Also for DNA2AP28 the quenching rate approximately doubles upon lowering the temperature, which can again be explained by hole transfer to two guanines in the opposing strand (it should be noted, however, that hole transfer to those additional guanines would imply that the value of p_1 is in fact even lower). Again, a quenching component of several tens of picoseconds is observed, which is ascribed to base reorientation. In addition, a component of several hundreds of picoseconds is present, which is probably due to reorientation of a larger part of the oligonucleotide.

Strikingly different results are obtained for DNA2AP21. It should be noted that 2AP is not base paired in the representation in Fig. 2. A fast quenching time is observed like for DNA2AP10, but the contribution is significantly smaller, although the number and distance of nearby guanines is the same as for DNA2AP10 (1 base and 2 bases away). However, also a lifetime of ~10 ns is observed, with a large contribution (0.44), indicating that a large fraction of the oligonucleotide adopts a conformation where 2AP does not stack at all with neighboring bases. It was shown by Peterson and Feigon (1996) using NMR that RBE3 adopts a conformation where the adenine at position 21 loops out completely, whereas both neighboring bases (20 and 22 in our case) stack upon each other. According to our data such a conformation also occurs for 2AP in DNA2AP21 (and most likely for adenine at position 21 in the other studied oligonucleotides), but it coexists with a conformation where nucleotide 21 is stacked with at least one neighboring base. Obviously, the difference in distance between G20 and 2AP in the looped-out conformation as compared with the stacked conformation cannot completely explain the enormous difference in hole transfer rates (~10 ns vs. ~10 ps). Besides a distance dependence, a correlation between the overlap of the π orbitals between donor and acceptor must play an important role for the transfer rate.

A somewhat similar situation occurs for DNA2AP26, which does not base pair. Also in that case a slow component of many nanoseconds is present, but its contribution is much smaller (0.08 vs. 0.44). This is readily understood because one neighbor (T25) does also not form a base pair (unlike both neighbors of DNA2AP21), and therefore the tendency to loop out is less strong. It should be noted that the fast quenching rates for DNA2AP26 and DNA2AP21 are identical at room temperature and 80°C, unlike those of DNA2AP28 and DNA2AP10 where 2AP forms a base pair, and this agrees with the hypothesis above that in these latter DNAs in the stacked base-paired configuration the hole

transfer can occur to guanines in the opposing strand in the latter two cases.

Time-resolved anisotropy measurements

We first discuss the anisotropy for DNA2AP21 at room temperature. The fastest component is 140 ps (amplitude 0.20). This corresponds to a large extent to depolarization of 2AP that is in the looped-out conformation, because the stacked conformation has a fluorescence lifetime of only 10 ps and does not contribute to the fluorescence on the time scale of depolarization. Because the sugar of 2AP is immobilized in the sugar-phosphate backbone, depolarization is expected to be mainly due to rotation of the base around the glycosidic bond. The rotational correlation time is of the same order of magnitude as that of free 2APR (80 ps), and the rotation is apparently hindered to some extent (both in time and space), probably by the restriction of the fixed glycosidic bond and/or the environment of the oligonucleotide, which is most likely somewhat more ordered than the water environment of 2APR when it is free in solution. The slow depolarization (1.8 ns, amplitude 0.16) is ascribed to a combination of overall bending, twisting, and rotational diffusion around several axes. All these processes have their own characteristic rates and amounts of depolarization, but resolving these is beyond the possibilities of the current measurements. Earlier results by Nordlund et al. (1989) in which 2AP was either base paired with another 2AP or adenine reported a short anisotropy time of, respectively, ~150 ps (amplitude of 0.092) and ~180 ps (amplitude of 0.128) at 25°C, which is comparable to the times we obtain considering both the decay times and the amplitudes. Guest et al. (1991) report a rotational correlation time of ~80 ps with an amplitude of 0.21 (the average for each of the different possible counter bases T, G, A, and C) at 20°C, a time constant somewhat faster then we find at 24°C, indicating faster motion of the 2AP. Both studies (Nordlund et al., 1989; Guest et al., 1991) report additional nanosecond components, also reflecting a combination of overall bending, twisting, and rotational diffusion.

The amount of depolarization is 0.20, and if it is entirely due to complete rotation around the glycosidic bond, the expected depolarization would be 0.33 using the values for the orientation of the lowest energy transition dipole of 2AP as obtained by Holmén et al. (1997) (see Appendix for detailed calculations). Hence it is concluded that the looped-out nucleotide experiences hindrance to rotate completely around its glycosidic bond. Similar results are obtained for DNA2AP26 (τ = 150 ps and 2 ns). Whereas for DNA2AP21 the fastest depolarization time corresponds predominantly to the conformation in which 2AP is completely looped out (this conformation corresponds to τ_4 and dominates the fluorescence intensity on the time scale of depolarization), for DNA2AP26, the contribution of τ_4 is far less (8%) and even smaller than that of τ_3 (11%, Table 1). Note

that τ_2 is significantly faster, and the corresponding conformation hardly contributes to the observed depolarization. The depolarization time depends strongly on the temperature. For molecules in solution the rotational time scales with η/kT, where η is the viscosity, k Boltzmann's constant, and T the temperature (Cantor and Schimmel, 1980), and for a molecule in water one expects a decrease in time with a factor of 1.74 upon going from 24°C to 58°C and a factor of 3.48 upon going from 24°C to 80°C. Using these factors, one expects a decrease from 145 (average of 140 and 150 ps) to 83 ps at 58°C and 42 ps at 80°C. This is close to the observed values (80 ps and 40 ps for DNA2AP21 and 60 ps and 30 ps for DNA2AP26), consistent with the idea that 2AP can loop out into the water environment. It is of interest to see that the depolarization time of 2AP in DNA2AP28 is slower at room temperature, pointing to hindered motion (not looped out), but at 58°C and 80°C the rotation occurs with a similar time constant as that of DNA2AP26, indicating a similar freedom to move. Because of the high amount of quenching at 24°C, no reliable rotational correlation times for DNA2AP10 could be obtained. A very fast rotational correlation time of 22 ps is observed for DNA2APIN at 20°C, but the corresponding contribution is very low (0.05), which might indicate a very restricted motion. At the highest temperature the fast rotational times of all complexes are very similar, which is readily explained by the melted structure in which all bases have the same motional freedom.

At room temperature all slow depolarization times are rather similar, ~2 ns. The slow time of 2 ns most likely reflects a combination of overall rotation, bending, and twisting of the oligonucleotides (see above). The average rotation time of DNA2AP21, DNA2AP26, and DNA2AP28 is 2.0 ns (for DNA2AP10 it could not be determined due to the fast quenching). Without structural changes one might expect a decrease to ~1.1 ns at 58°C (with the temperature dependence given above), and the observed times for DNA2AP10 (0.8 ns) and DNA2AP21 (0.9 ns) are relatively close, albeit that they are somewhat smaller than expected. However, for DNA2AP26 and DNA2AP28 they are much smaller, namely, 0.4 ns. This shows increased mobility in the region close to the 5′ and 3′ ends of the oligonucleotides, suggesting (partial) melting in this region. It should be noted that at 58°C the melting of the hairpin is not complete (~50%), and these results indicate that melting starts at the ends of the hairpin. At 80°C the hairpin is completely melted out and the rotational times are again very similar to each other (namely, 0.2 ns). Based on the simple temperature dependence given above the slow depolarization time would have been 0.6 ns in the absence of denaturation (2.0ns/3.48; see above). The idea of local melting is also consistent with the value of the fast depolarization times at 58°C, which are found to be shorter for DNA2AP26 and DNA2AP28 than for DNA2AP10 and DNA2AP21. It was mentioned above that at room temperature, the fast depo-

larization of DNA2AP21 is mostly due to the looped-out conformation (not the stacked one). However, at 58°C the situation has changed because the relative contribution of this conformation has decreased and more interconversion with the stacked conformation occurs; ratio of the contribution of τ_4/τ_3 decreases from 11 to 1.7.

CONCLUSIONS

Using time-resolved (polarized) fluorescence spectroscopy on DNA hairpins that were site-selectively substituted with the fluorescent adenine analog 2AP, several structural and dynamical features of the DNA hairpin structure could be revealed.

Structural heterogeneity of the DNA hairpin was demonstrated by the extraction of four isotropic fluorescence decay times, corresponding to different degrees of quenching of the 2AP fluorescence. We suggest this quenching to be due to hole transfer from 2AP to guanine, and it could be well described using a simple model based on the probability of stacking of neighboring bases. Besides intra-strand hole transfer there are strong indications for significant inter-strand hole transfer in the base-paired hairpin.

Heterogeneity is particularly clear for DNA2AP21 where a stacked and a looped-out conformation coexist. The disorder in the DNA was illustrated by the fact that even for double-stranded regions, the probability of stacking for neighboring bases seems to be only ~75%.

Both dynamics of the entire DNA as well as local dynamics were reflected in the fluorescence anisotropy data, although the signal-to-noise ratio is not high enough to allow detailed interpretations. Besides isotropic times of ~8 ps reflecting direct hole transfer and >1 ns representing conformations unfavorable for transfer, two intermediate isotropic times were found. These times of ~50 ps and ~500 ps represent either conformations that reorganize before quenching can occur or conformations leading to slow quenching.

By studying the polarized fluorescence decay as a function of temperature, the dynamics of the melting process could be investigated. The results strongly indicate local melting; initially, the C-N terminal end of the hairpin melts, whereas the remaining part of the hairpin starts to melt only at higher temperatures.

APPENDIX

Modeling of the observed quenching rates

For DNA2AP10 at 80°C (complete denaturation), eight (2^3) situations (for bases G8, C9, 2AP10, and G11) for the orientation of the bases with respect to their neighbors can be distinguished, if two mutual orientations are assumed for two neighboring bases (stacked and unstacked). The probability that neighboring bases are stacked is called p_1, and hence the probability that two neighboring bases do not stack is equal to $1 - p_1$. The total quenching rate of 2AP is denoted by k_0. The quenching rate of 2AP

TABLE 4 Calculated quenching rates k_0 with corresponding probabilities A_0 for DNA2AP10 assuming one quenching process (see Appendix)

A_0	k_0
$(1 - p_1)^3$	0
$p_1(1 - p_1)^2$	0
$p_1(1 - p_1)^2$	0
$p_1^2(1 - p_1)$	k_1
$p_1(1 - p_1)^2$	k_1
$p_1^2(1 - p_1)$	k_1
$p_1^2(1 - p_1)$	k_1
p_1^3	$2k_1$

due to one guanine is denoted by k_1 and the rate due to two guanines (on both sides) is $2k_1$. The situations that can occur, with the corresponding probabilities A_0, are given in Table 4.

The sum of all the probabilities for the slow components (τ_2, τ_3, τ_4), X, is $(1 + p_1)(1 - p_1)^2$. The contribution of the fast component is therefore $1 - X = 1 - (1 + p_1)(1 - p_1)^2$. This model can explain the decay rates with their corresponding contribution for both DNA2AP10 and DNA2AP21 at 80°C if a probability of $p_1 = 0.39$ is used. However, an additional fast quenching process with rate k_2 has to be taken into account to describe all the magic-angle decay data consistently. This fast quenching process has a certain probability p_2 to occur; the DNA should have the right conformation for this process. Importantly, the additional fast quenching process does not occur in all conformations, because otherwise the contribution of the fast component in the data would always equal one ($p_2 \neq 1$). If an additional independent quenching process is taken into account, the contribution for the slow components has to be multiplied by $(1 - p_2)$. Table 5 presents the calculated results obtained for DNA2AP10 using $p_1 = 0.25$ and $p_2 = 0.28$.

The observed rate will now be approximately equal to $[0.197k_2 + 0.214k_1 + 0.08(k_1 + k_2)]/[0.197 + 0.241 + 0.08] = 10$ ps^{-1} for DNA2AP10 and DNA2AP21. For DNA2AP28 the contribution of k_1 is negligible, so $k_2 = (20$ ps$)^{-1} = 50$ ns^{-1} (the first quenching process is negligible for this DNA because fitting the data only with k_1 gives a much too low contribution for the fast component). From these two equations it follows that $k_1 = 128$ ns^{-1}. Using this model, the magic-angle data at 80°C for all the 2AP-substituted DNA oligodeoxynucleotides can be described as illustrated in Table 3.

When going to lower temperatures, the contribution of the fast component for DNA2AP10 increases dramatically up to 90%. Obviously, the probability of stacking is very much enhanced in this more rigid hairpin structure. If one assumes that the probability p_2 for the additional quenching process does not change, it turns out that the upper limit for p_1 is 0.72 for the bases around the 10 position. This value represents the disordered structure of the DNA hairpin; the probability that two neighboring bases will stack is only 72%, even at room temperature. If one assumes that p_2 becomes equal to 0, the probability for stacking goes up only a little bit to 75%.

TABLE 5 Calculated quenching rates with corresponding contributions for DNA2AP10 assuming two quenching processes using $p_1 = 0.25$ and $p_2 = 0.28$

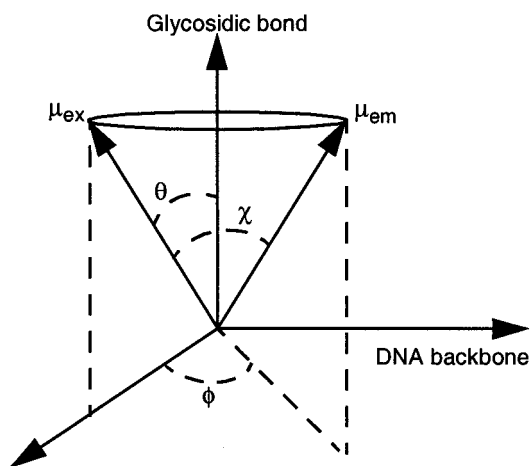| A_0	k_0	Relative contribution
$X(1 - p_2)$	Very slow	0.506
Xp_2	k_2	0.197
$(1 - X)(1 - p_2)$	k_1	0.214
$(1 - X)p_2$	$k_1 + k_2$	0.08

FIGURE 8 Definition of the angles that define the orientations of the absorption-dipole moment (μ_{ex}) and the emission-dipole moment at time t after excitation (μ_{em}).

Calculation of the fast anisotropy time for DNA2AP21

The anisotropy is given by (Cantor and Schimmel, 1980):

$$r(t) = \tfrac{1}{5}\langle 3\cos^2\chi(t) - 1\rangle = \tfrac{3}{5}\langle\cos^2\chi(t)\rangle - \tfrac{1}{5}, \quad (4)$$

with χ the angle between the absorption and emission dipole moment. In 2AP, these are known to be almost parallel (Holmén et al., 1997). However, after excitation the probe can rotate around its glycosidic bond, which gives rise to an angle χ between the absorption dipole moment at time 0 and the emission dipole moment at time t. The value of $\cos\chi$ can be calculated using Fig. 8:

$$\cos\chi = \cos^2\theta + \sin^2\theta\cos\phi \quad (5)$$

Hence, if depolarization is entirely due to free rotation around the glycosidic bond, the final anisotropy will be

$$r = \tfrac{3}{5}(\cos^4\theta + \tfrac{1}{2}\sin^4\theta) - \tfrac{1}{5} \quad (6)$$

(i.e. all values for ϕ are equally likely to occur). The measured value of the depolarization of the fast component is 0.20. The value of θ can be estimated from the literature (Holmén et al., 1997) and is $\sim$39°, which gives rise to an anisotropy of 0.07.

REFERENCES

Briki, F., J. Ramstein, R. Lavery, and D. Genest. 1995. Rotational motions of bases in DNA. *In* Modelling of Biomolecular Structures and Mechanisms. A. Pullman, editor. Kluwer Academic Publishers, Dordrecht, The Netherlands. 231–239.

Broo, A. 1998. A theoretical investigation of the physical reason for the very different luminescence properties of the two isomers adenine and 2-aminopurine. *J. Phys. Chem. A.* 102:526–531.

Broo, A., and A. Holmén. 1996. Ab initio MP2 and DFT calculations of geometry and solution tautomerism of purine and some purine derivatives. *Chem. Phys.* 211:147–161.

Bruant, N., D. Flatters, R. Lavery, and D. Genest. 1999. From atomic to mesoscopic descriptions of the internal dynamics of DNA. *Biophys. J.* 77:2366–2376.

Cantor, C. R., and P. R. Schimmel. 1980. Biophysical Chemistry, Part 2. W. H. Freeman, New York.

Eggeling, C., J. R. Fries, L. Brand, R. Günther, and C. A. M. Seidel. 1998. Monitoring conformational dynamics of a single molecule by selective fluorescence spectroscopy. *Proc. Natl. Acad. Sci. U.S.A.* 95:1556–1561.

Farrer, B. T., and H. H. Thorp. 2000. Redox pathways in DNA oxidation: kinetic studies of guanine and sugar oxidation by para-substituted derivatives of oxoruthenium(IV). *Inorg. Chem.* 39:44–49.

Frauenfelder, H., S. G. Sligar, and P. G. Wolynes. 1991. The energy landscapes and motions of proteins. *Science.* 254:1598–1603.

Georghiou, S., T. D. Bradrick, A. Philippetis, and J. M. Beechem. 1996. Large-amplitude picosecond anisotropy decay of the intrinsic fluorescence of double-stranded DNA. *Biophys. J.* 70:1909–1922.

Grove, A., A. Galeone, L. Mayol, and E. P. Geiduschek. 1996. Localized DNA flexibility contributes to target site selection by DNA-bending proteins. *J. Mol. Biol.* 260:120–125.

Guest, C. R., R. A. Hochstrasser, L. C. Sowers, and D. P. Millar. 1991. Dynamics of mismatched base pairs in DNA. *Biochemistry.* 30:3271–3279.

Hagerman, P. J. 1988. Flexibility of DNA. *Annu. Rev. Biophys. Biophys. Chem.* 17:265–286.

Hochstrasser, R. A., T. E. Carver, L. C. Sowers, and D. P. Millar. 1994. Melting of a DNA helix terminus within the active site of a DNA polymerase. 1979. *Biochemistry.* 33:11971–1.

Hogan, M. E., and R. H. Austin. 1987. Importance of DNA stiffness in protein-DNA binding specificity. *Nature.* 329:263–266.

Holmén, A., B. Nordén, and B. Albinsson. 1997. Electronic transition moments of 2-aminopurine. *J. Am. Chem. Soc.* 119:3114–3121.

Kelley, S. O., and J. K. Barton. 1999. Electron transfer between bases in double helical DNA. *Science.* 283:375–381.

Kingsman, S. M., and A. J. Kingsman. 1996. The regulation of human immunodeficiency virus type-1 gene expression. *Eur. J. Biochem.* 240:491–507.

Kleima, F. J., E. Hofmann, B. Gobets, I. H. M. van Stokkum, R. van Grondelle, K. Diederichs, and H. van Amerongen. 2000. Förster excitation energy transfer in pyridinin-chlorophyll-a-protein. *Biophys. J.* 78:344–353.

Lacourciere, K. A., J. T. Silvers, and J. P. Marino. 2000. Mechanism of neomycin and rev peptide binding to the rev responsive element of HIV-1 as determined by fluorescence and NMR spectroscopy. *Biochemistry.* 39:5630–5641.

Lehninger, A. L. 1976. Biochemistry. Worth Publishers, New York.

Naimushin, A. N., B. S. Fujimoto, and J. M. Schurr. 2000. Dynamic bending rigidity of a 200-bp DNA in 4 mM ionic strength: a transient polarization grating study. *Biophys. J.* 78:1498–1518.

Nordlund, T. M., S. Andersson, L. Nilsson, R. Rigler, A. Gräslund, and L. W. McLaughlin. 1989 Structure and dynamics of a fluorescent DNA oligomer containing the *Eco*RI recognition sequence: fluorescence, molecular dynamics, and NMR studies. *Biochemistry.* 28:9095–9103.

Nordlund, T. M., D. Xu, and K. O. Evans. 1993. Excitation energy transfer in DNA: duplex melting and transfer from normal bases to 2-aminopurine. *Biochemistry.* 32:12090–12095.

Parkhurst, K. M., and L. J. Parkhurst. 1995. Donor-acceptor distributions in a double-labeled fluorescent oligonucleotide both as a single strand and in duplexes. *Biochemistry.* 34:293–300.

Peterson, R. D., and J. Feigon. 1996. Structural change in rev responsive element RNA of HIV-1 on binding rev peptide. *J. Mol. Biol.* 264:863–877.

Richmond, T. J., J. T. Finch, B. Rushton, D. Rhodes, and A. Klug. 1984. Structure of the nucleosome core particle at 7 Å resolution. *Nature.* 311:532–537.

Schurr, J. M., B. S. Fujimoto, P. Wu, and L. Song. 1992. Fluorescence studies of nucleic acids: dynamics, rigidities, and structures. *In* Topics in Fluorescence Spectroscopy, Vol. 3. J. R. Lakowicz, editor. Plenum Press, New York. 137–229.

Shafirovich, V., A. Dourandin, W. Huang, N. P. Luneva, and N. E. Geacintov. 1999. Oxidation of guanine at a distance in oligonucleotides induced by two-photon photoionization of 2-aminopurine. *J. Phys. Chem. B.* 103:10924–10933.

Shafirovich, V., A. Dourandin, W. Huang, N. P. Luneva, and N. E. Geacintov. 2000. Electron transfer at a distance induced by site-selective photoionization of 2-aminopurine in oligonucleotides and investigated by transient absorption techniques. *Phys. Chem. Chem. Phys.* 2:4399–4408.

Sowers, L. C., G. V. Fazakerley, R. Eritja, B. E. Kaplan, and M. F. Goodman. 1986. Base pairing and mutagenesis: observation of a protonated base pair between 2-aminopurine and cytosine in an oligonucleotide by proton NMR. *Proc. Natl. Acad. Sci. U.S.A.* 83: 5434–5438.

Steenken, S., and S. V. Javonavic. 1997. How easily oxidizable is DNA? One-electron reduction potentials of adenosine and guanosine radicals in aqueous solution. *J. Am. Chem. Soc.* 119:617–618.

van Stokkum, I. H. M., H. Linsdell, J. M. Hadden, P. I. Haris, D. Chapman, and M. Bloemendal. 1995. Temperature-induced changes in protein structures studied by Fourier transform infrared spectroscopy and global analysis. *Biochemistry.* 34:10508–10518.

van Stokkum, I. H. M., T. Scherer, A. M. Brouwer, and J. W. Verhoeven. 1994. Conformational dynamics of flexibility and semirigidly bridged electron donor-acceptor systems as revealed by spectrotemporal parameterization of fluorescence. *J. Phys. Chem.* 98:852–866.

Wan, C., T. Fiebig, S. O. Kelley, C. R. Treadway, J. K. Barton, and A. H. Zewail. 1999. Femtosecond dynamics of DNA-mediated electron transfer. *Proc. Natl. Acad. Sci. U.S.A.* 96:6014–6019.

Wan, C., T. Fiebig, O. Schiemann, J. K. Barton, and A. H. Zewail. 2000. Femtosecond direct observation of charge transfer between bases in DNA. *Proc. Natl. Acad. Sci. U.S.A.* 97:14052–14055.

Wolffe, A. P. 1994. Architectural transcription factors (comment). *Science* 264:1100–1101.

Wu, P., T. M. Nordlund, B. Gildea, and L. W. McLaughlin. 1990. Base stacking and unstacking as determined from a DNA decamer containing a fluorescent base. *Biochemistry.* 29:6508–6514.